Transportation Research Interdisciplinary Perspectives 20 (2023) 100846

Contents lists available at ScienceDirect

Transportation Research Interdisciplinary Perspectives

journal homepage: www.elsevier.com/locate/trip

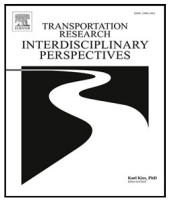

Forwarding containers to dry ports in congested logistic networks

Anna Sciomachen [a], Giuseppe Stecca [b,*]

[a] Department of Economics and Business Studies, University of Genoa, Via Vivaldi 5, 16126 Genova, Italy
[b] Institute of Systems Analysis and Computer Science of National Research Council CNR-IASI, Via dei Taurini 19, 00185 Roma, Italy

ARTICLE INFO

Keywords:
Maritime logistics
Container inland forwarding
Multi-commodity flow function
Congestion
Time dependent travel cost function

ABSTRACT

This work investigates the impact of container arrival flow rate on the port surrounding network and proposes a mixed integer programming model to optimize their forwarding towards dry port destinations. A novel efficient model with limited network capacity and time period dependent travel cost function is proposed. The aim is to give a decision support for operational planning with limited capacity of both the terminal yard and the logistic network, with respect to the quantity of containers transferred per time unit. The model considers time dependent costs and traveling times to reduce congestion. As a further novel issue of the model, arc costs and traveling times change during specific time slots. More precisely, new linear functions are derived as tangents to the nonlinear convex components of a classical traveling time function proposed in the literature. The aim is to produce a light model which can be effectively used for macro planning of forwarding operations. The model is proved to be fast in real case instances also if compared to classical literature approaches. The model is used to study the container dispatching process in a terminal which is going to be the main Italian container terminal equipped to manage mega-ship traffic. Results obtained from real-size instances are reported. We tested the behavior of the model under different scenarios. Our tests confirmed model efficiency and its of supporting the management of peak events also by controlling shut-down time slots to lower congestion.

1. Introduction

Container vessels account for about a quarter of the world's total fleet and are therefore essential for the international transport of goods. The massive development of multilateral trade gave rise to the development of the maritime sector, fostering technological innovations such as digitization and naval gigantism. Since the outbreak of the Covid-19 pandemic and the Russian–Ukrainian conflict that erupted in February 2022, maritime transport has experienced a severe crisis globally, causing container shortages, rising container charter prices, port congestion and days of ship delays. Thus, an increase in direct and external costs for ports and their hinterland was inevitable. To maintain business continuity and sustainability, several actions need to be adopted in terms of infrastructural and technological adaptations of ports, by the handling operations authorities, in order manage properly the peak port congestion and mitigate environmental impacts (Haralambides, 2019).

However, congestion problems existed even before the mentioned crisis. In fact, many ports are inefficient and cannot cope with the traffic generated by the high demand for goods, and most of them have proved unsuitable for accommodating mega ships, and to dispatch effectively peak flows (Medina et al., 2021). One of the main problems seaports face today are the lack of space at maritime terminals and the growing congestion on their access routes with the inland connections, especially with respect to the road modality (De Langen and Chouly, 2004). Both criticalities risk to nullify the efforts of terminal operators in the optimization of quayside and yard operations, making difficult to handle thousands of unloaded containers from the yard to the required destinations in short time (Kramberger and Monios, 2018; Notteboom and Rodrigue, 2008; Essel et al., 2022). Since congestion represent a direct cause of these port problems, it is extremely important to take into account the value of negative externalities in the design and management of freight transport networks, as highlighted in the work of Tawfik and Limbourg (2019). In this direction, recently a lot of research works have been proposed (see, among others, Kurtuluş (2022)).

To cope with this need and the technological demands of containerization worldwide, the port industry has invested significantly. Modern container terminals have been built and new, more efficient organizational forms have been adopted to speed up port operations (Haralambides, 2019; dos Santos and Pereira, 2021; Feng et al., 2023). Therefore, it is necessary to analyze the trade-offs between the benefits offered by novel technological trends (e.g. mega containerships) and their cost over the entire transport chain, including pollution and traffic congestion of the inland transportation networks (Kurt et al., 2021).

* Corresponding author.
E-mail address: giuseppe.stecca@iasi.cnr.it (G. Stecca).

https://doi.org/10.1016/j.trip.2023.100846
Received 7 November 2022; Received in revised form 2 April 2023; Accepted 17 May 2023
Available online 31 May 2023

Starting for the last decade, many authors proposed the use of dry ports and hub & spoke networks to improve performances and the competitiveness of inland shipping. Suggested works are, among others, by Gelareh et al. (2010) and Roso and Lumsden (2010). In this scenario, the importance of ports as international logistic nodes will increase further. In this context, it is strongly required to promote transport policies able to shift shares of assigned volumes to road transport to other modalities. However, in many countries, in particular in Italy, road transport is still the most convenient shipping modality (Mostert et al., 2017; Notteboom and Rodrigue, 2008). Therefore, especially with the current focus on environmental sustainability, there is the need to consider the social costs derived from such a high increasing volume of goods traveling every day on the main highway connections, merging them with the private and commercial vehicles. In this direction, a number of research works focused on evaluating the negative impact of high volumes of containerized flows shipped by using the road modality have been proposed (Ambrosino et al., 2019; Brandenburg et al., 2014; Korzhenevych et al., 2014; Petro and Konečnỳ, 2017).

In this paper, we consider a road transportation network connecting ports to inland destinations with the limitations given by the network and the vehicles availability as in Ambrosino et al. (2018) and Di Francesco et al. (2019). We propose a mathematical programming model to optimize the containers forwarding towards possible dry ports and final destinations. The remainder of this work is as follows.

Section 2 refers to the presentation of the research problem. In Section 3 we described the proposed model and its linear formulation to face the considered problem. The application case study is described in Section 4, while in Section 5 results and comparisons are presented. Section 6 concludes the paper and gives outlines for future works.

2. Research problem definition

In this section we present the addressed research problem. The aim is to reduce the congestion in the road transportation network connecting seaports to the hinterland. To this end, we propose a mathematical programming model to optimize the forwarding of containers to possible dry ports and final destinations. The idea is to provide a decision support for operational planning in the presence of limited capacity in both the yard of the terminal for container storage and the network due to the quantity of containers transferred per time unit. Other research works have been recently proposed in this direction. In particular, Sterzik and Kopfer (2013) propose a tabu search heuristic for a trucking company with a homogeneous fleet to receive inbound containers or ship outbound ones. Funke and Kopfer (2016) present a mixed integer linear programming model for dispatching 20-, and 40-feet containers, with the aim of minimizing either the traveling distance or the operation time of the different types of trucks involved in the transportation process. More recently, Jia et al. (2022) proposed a Markov decision-making model to deal efficiently with uncertain demands of container transport in a dynamic way.

As a novel issue, our proposed model considers costs depending on the traveling times varying according to the amount of flow on the network. Further, the minimization of the road congestion is measured by the sum of the flow of container trucks multiplied by the arc traveling time associated with each arc of the network. The purpose is to consider in the decisions the reduced capacity of the road transport network that could result in congestion, especially in the links originating from the ports. In particular, we include in the model a possible delay in the departing time of the vehicles from the origin ports as soon as a congestion levels on the surrounding arcs is close to given threshold values. Shipment delays have been previously considered by Ishfaq and Sox (2012) with the aim to explore the effect of limited resources and modal transit time variability on hub networks in the presence of service time requirements. Further, Yu et al. (2018) proposed a two-phase game model to study the ocean carrier's decision about the free detention time and the time when the container arrived at the inland terminal is dispatched to the sea container terminal. Karimi-Mamaghan et al. (2020), consider the congestion in both hubs and connection links, using queuing theory, and focus on the minimization of waiting times. Waiting times are also considered by Wang et al. (2020), where congestion affects waiting time. Jia et al. (2020) proposed a simulation–optimization approach for the optimal scheduling of deep-sea vessel berth planning and feeder arrival. In this paper, container allocation strategies are proposed to maximize revenue under time sensitive and dynamic pricing of container slots. Li et al. (2022) uses an equilibrium model to solve a bottleneck congestion problem for containerized freight flows by taking into account various supply and demand characteristics existing in the China–Europe freight transportation market. Congestion, in our work is modeled as dependent traveling time for arcs. Moreover, differently by the cited approaches, the application is to the gate and the port surrounding area, so it is a first mile problem, where the objective function is the minimization of the congestion measured as time spent on the network by the carriers. The presented model allows us to analyze the containers dispatching process in a case study derived from APM-VL (Vado Ligure) which is going to be the main Italian container terminal equipped to manage mega-ship traffic; APM-VL container terminal is part of the Port Authority of the Western Ligurian Sea, which also includes the ports of Genoa, Savona and Pra. The terminal is active from the second half of December 2019. Excluding the traffic variation observed from 2020 as a result of the effects of the covid-19 pandemic, the expected throughput of the terminal, expressed in terms of the number of containers handled per year, is about 800,000 TEUs. The main performance indices of the terminal under consideration have been recently analyzed in Musso and Sciomachen (2020) by using a discrete event simulation study considering different ship arrival profiles. In the present work, the output performance indices data derived from Musso and Sciomachen (2020) are considered for tuning the origin–destination containerized ow demand in different daily time periods.

The literature on network flows and congestion analysis and optimization considers different modeling approaches based on equilibrium problem, simulation, and optimization. As for the approach proposed in our work, one key milestone is the work of Merchant and Nemhauser (1978) that modeled the congestion caused by vehicles over a network flow, and congestion costs are minimized in a nonlinear formulation. In the model, the objective function is the minimization of the sum of non-negative, non-decreasing, continuous, convex functions depending on the flow for each arc in each given time period. Congestion is represented by functions acting on ow balancing constraints (through travel time). These functions are considered as non-decreasing, continuous, concave and represent the physical phenomenon of congestion. In order to solve the model, the authors linearize them by means of piece-wise linear approximation. The model is single source and single sink. As reported by the survey of Peeta and Ziliaskopoulos (2001), the fundamental work of Merchant and Nemhauser (1978) has been expanded in several directions in terms of methodologies and applications. The principal methodologies used to study the dynamic equilibrium assignment problem are mathematical programming, variational inequality, optimal control, and simulation-based, while the most studied applications are the traffic assignment, real-time deployment, and planning. Carey (1992), Carey and Subrahmanian (2000) demonstrated the non-convexity of the dynamic traffic assignment problem and clarified several problems of the mathematical programming approach when dealing with FIFO. FIFO means that, in the mathematical programming models, no overtaking is allowed among vehicles traveling an arc. Holding-back is considered in real situations and it means to favor certain traffic movements over others in order to minimize system-wide travel delays. An interesting research direction has been the introduction of stochastic features or uncertainties. In particular, Birge and Ho (1993) extend the Merchant and Nemhauser (1978) problem and consider the stochastic case by assuming that the origin–destination matrix is not completely known for the entire planning

horizon. A control theory based approach is discussed by Papageorgiou (1990) who considers as variables the split rates in sub-flows, allowing the computation of route guidance information. Carey and Subrahmanian (2000) introduce another important achievement for this research line. In their single sink model the authors investigate the impact of capacity and the relation between link ow, trip time and cost. Other extensions of the problem are related to different applications, as for example the one of Alizadeh et al. (2014) where the problem of electric vehicle routing and charging is discussed.

3. Focus on the proposed mathematical models and explanations

In this section we introduce a linear programming based approach to plan the dispatching of containers from the port to the destinations with the aim of minimizing congestion. We take the approach of mathematical programming and consider a more appropriate network flow model in which capacity constraints are considered for nodes and arcs while multi-sinks are modeled. The main issue when planning containers forwarding is to consider if the traveling time is or not dependent on the flow that is going to plan. Probably the most famous model of travel time is the Bureau of Public Roads (BPR) (Manual, 1964) function, which considers the travel time as dependent by the flow q with the following polynomial relation:

$$\tau = T_{ff}\left[1 + \alpha\left(\frac{q}{q_{pc}}\right)^{\beta}\right] \tag{1}$$

Function (1) defines the traveling time τ of one arc with maximum capacity of q_{pc} when a flow q is present; α and β are parameters, T_{ff} is the traveling time when free flow is considered. The function is almost flat before the threshold β is reached, then it starts to increase significantly (Maerivoet and De Moor, 2005).

This function is the base of several convex optimization problems with the aim to solve the traffic equilibrium problem. Often, flow dependent or time dependent travel times should be considered in settings with more general planning problems. In these settings, the nonlinear parameter can be addressed in several ways in order to reduce the complexity, and the particular shape of the BPR function allows a straightforward piece-wise approximation.

3.1. The linear programming model

Having in mind the traveling time equation given in (1), we propose a new model aimed at minimizing the total traveling time spent by all trucks along arcs of a given graph G within the planning time horizon $\mathcal{H}$.

We assume that $\mathcal{H}$ starts with the arrival of the mega-ship holding the containers to be delivered and ends with the delivery of all containers to the required destinations by the given g days.

The other following assumptions apply.

Assumption 3.1. The flows generated by the trucks have no considerable effect on the traveling time in the time slot considered.

Observation 3.1. *Assumption 3.1 means that we can consider a multi-period linear model. This is important because the decision maker can act to dispatch the schedules of forwarding in order to lower the congestion on the network in a short/medium time horizon. To model this situation the planning horizon $\mathcal{H}$ is discretized into T time slots; the traveling time on the network varies during this time horizon, but it is independent of the output flow of the decision model.*

Assumption 3.2. The number of containers required to be moved can be easily translated in a number of trucks used; in particular, a twenty TEU truck can transport only 1 twenty feet container, while forty feet truck can have either 2 twenty feet container or 1 forty feet container.

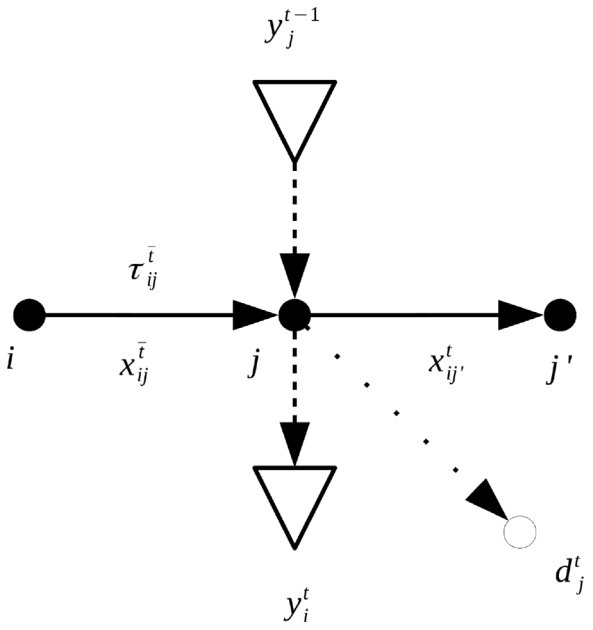

Fig. 1. Exemplification of a node of the network.

The considered road transportation network is represented as an oriented graph $G = (N, A)$ where N is the set of nodes, which includes origins, destinations and transit nodes, and A is the set of directed arcs representing the existing road connections. For each node $j \in N$ and each time slot $t \in T$, a required demand d_j^t of containers is given.

The demand should be delivered from the source $s \in N$, which corresponds to the unloading point of the port and where a quantity $-d_s^t$ must be forwarded during the time horizon, such that $-\sum_{t\in T} d_s^t = \sum_{j\in N\setminus s, t\in T} d_j^t$. Another parameter considered in the model is the traveling time τ_{ij}^t, $\forall t \in T$, $\forall (i,j) \in A$, given for each arc of the network and for each time slot of the planning horizon, that is the traveling time encountered by a truck entering arc (i,j) at timeslot t.

Assumption 3.3. The value τ_{ij}^t of the traveling time is defined in terms of numbers (integer ≥ 1) of time slots, since it is considered to be divisible by the single time slot.

Example 3.1. For example, if we divide the time horizon in time slots of 15 min, the traveling time of 60 min will be equal to $\tau_{ij}^t = 4$.

The objective of the problem is to minimize the total time spent on the arcs of the network by the containers to reduce the contribution to congestion. Congestion can be reduced through the availability of buffer zones where containers can be "parked" on their route to destination, or by delaying their shipping. Each node $j \in N$ is associated with a buffer with limited capacity cap_j. For nodes corresponding to dry ports this capacity is greater than zero while for all other network nodes the capacity will be set to zero. Capacity is also considered for the arcs. So, for each arc $\forall (i,j) \in A$ and for each time slot $t \in T$, a maximum number of trucks allowed to travel that arc is given and denoted with capA_{ij}^t. The given parameter is time dependent.

Defined the network and the parameters of the problem, in the proposed model, we consider the following decision variables:

- x_{ij}^t, is the number of containers (trucks) entering arc (i,j) during time slot t;
- y_j^t is the number of containers (trucks) in the buffer of node j in time t.

Fig. 1 reports a schema of the network flow and the related parameters and variables. The nodes are depicted as points, arrows denote

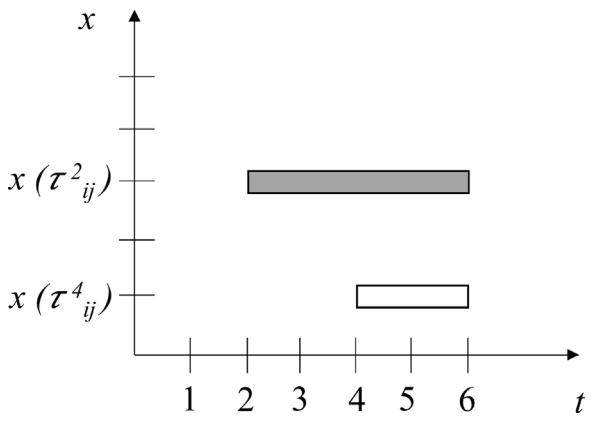

Fig. 2. Exemplification of trucks arriving from a node i to a node j at the same time 6. 3 trucks (gray box) depart at time 2 and encounter a travel time $\tau^2_{ij} = 4$, with (6 - τ^2_{ij}) = 2. Moreover, 1 truck (white box) departs at time 4 and encounter a travel time $\tau^4_{ij} = 2$, with (6 - τ^4_{ij}) = 4.

flows, while the overturned triangle depicts a buffer node - a node of the network where containers can be temporarily stored, as for example a dry-port - and the dashed arrow denotes the demand d^t_j of the corresponding outgoing node to be satisfied. The figure schematizes the flow balancing equation. The flow $x^{\bar{t}}_{ij}$ arriving to a given node j is defined for i direct predecessors of j and for times $\bar{t}$ such that $(t-\tau^{\bar{t}}_{ij}) \geq 0$, with $\tau^{\bar{t}}_{ij}$ being the traveling time of arc (i, j) at time $\bar{t}$. Therefore it holds that the sum of the flows $x^{\bar{t}}_{ij}$ entering the node j, plus y^{t-1}_j minus y^t_j, must be equal to the number of containers used to satisfy d^t_j plus the sum of the flow exiting from j and entering to nodes j' at time t, where j' are all the direct successors of j. The Fig. 2 shows an example of the notation introduced. It should be noted that a greater number of trucks traveling through the arc corresponds to a longer travel time.

The proposed model, in the afterwards named P0, can be then written as follows:

Model **P0**

$$\min \quad Z = \sum_{t\in T}\sum_{(i,j)\in A} \tau^t_{ij} x^t_{ij} \tag{2}$$

s.t.

$$\sum_{i\in\delta^-(j):\bar{t}=(t-\tau^{\bar{t}}_{ij})\geq 0} x^{\bar{t}}_{ij} + y^{t-1}_j = y^t_j + \sum_{k\in\delta^+(j)} x^t_{jk} + d^t_j \qquad j \in N, t \in T \tag{3}$$

$$0 \leq y^t_j \leq \text{cap}_i \qquad j \in N, t \in T \tag{4}$$

$$0 \leq x^t_{ij} \leq \text{capA}^t_{ij} \qquad (i,j) \in A, t \in T \tag{5}$$

$$y^t_j, x^t_{ij} \in \mathbb{Z}^{\geq 0} \qquad (i,j) \in A, t \in T \tag{6}$$

In model P0, Eq. (2) defines the objective function, meaning that the congestion is measured by the total traveling time spent by trucks on the network. Eqs. (3) represent the set of flow conservation constraints, which consider the travel time variable; the symbols $\delta^-(j)$ and $\delta^+(j)$ are the notations used to indicate the arcs entering and exiting a node j, respectively. Moreover, in the source the demand will be negative. Eqs. (4) defines the capacity constraints for buffers of each node, while (5) impose to the flow to respect the arcs capacity. Eqs. (6) specify the domain of the decision variables.

3.2. Modeling the traveling time

The traveling time of an arc can be considered as a scalar parameter only as first approximation. In this section we propose an improved model where Assumption 3.1 is removed and the following assumption is introduced.

Assumption 3.4. Traveling time is affected at least by 3 distinct features: (i) daytime t, (ii) type of arc (i, j), and (iii) flow x^t_{ij}.

While the first two features are represented in model P0 by parameter τ^t_{ij}, the third feature requires the introduction of a nonlinearity. In particular the BPR equation (1) is then considered and the new model, P1, becomes as follows:

Model **P1**:

$$\min Z = \sum_{t\in T}\sum_{(i,j)\in A} \tau^t_{ij} x^t_{ij} \tag{7}$$

s.t.

$$\sum_{i\in\delta^-(j):\bar{t}=(t-\tau^{\bar{t}}_{ij})\geq 0} x^{\bar{t}}_{ij} + y^{t-1}_j = y^t_j + \sum_{k\in\delta^+(j)} x^t_{jk} + d^t_j \qquad j \in N, t \in T \tag{3}'$$

$$0 \leq y^t_j \leq \text{cap}_i \qquad j \in N, t \in T \tag{4}'$$

$$0 \leq x^t_{ij} \leq \text{capA}^t_{ij} \qquad (i,j) \in A, t \in T \tag{5}'$$

$$\tau^t_{ij} = T_{ff}\left[1 + \alpha\left(\frac{x^t_{ij}}{q_{pc}}\right)^{\beta}\right] \qquad (i,j) \in \bar{A}, t \in T \tag{8}$$

$$y^t_j, x^t_{ij} \in \mathbb{Z}^{\geq 0} \qquad (i,j) \in A, t \in T \tag{6}'$$

In this updated model, Eq. (8) represents the nonlinearity affecting the objective function (7), through its definition. Model P1 can be linearized by a piece-wise linear approximation. The linearization can be done by upper, mean, or lower approximations. In the following, we describe a lower approximation by 1-degree linearization using tangents to each nonlinear convex term, and upper approximation using secants.

3.3. Lower approximation

Assumption 3.5. In order to linearize the objective function given in (7), we suppose $0 \leq x^t_{ij} \leq \text{capA}^t_{ij}$ to be continuous.

Observation 3.2. *The lower approximation can be done by tangents which can be easily computed because each objective function term $Z(x^t_{ij}) = \tau^t_{ij} x^t_{ij}$ is a $\beta + 1$ grade polynomial which is continuous and differentiable under Assumption 3.5.*

Definition 3.1. Let $\bar{A} \in A$ be the subset of arcs for which the traveling time τ^t_{ij} is assumed to be nonlinear. We define $\gamma^{tm}_{ij}, m = 1 \dots M$ the set of points where we linearize the objective function term, with $\gamma^{t1}_{ij} = 0$, and $\gamma^{tM}_{ij} = \text{capA}^t_{ij}$.

Definition 3.2. $\forall \bar{A} \in A$ we define the tuples $(a^{mt}_{ij}, b^{mt}_{ij}) \in M^t_{ij}$ such that the equations $a^m_{ijt}\gamma^{tm}_{ij} + b^{mt}_{ij} = Z(\gamma^{tm}_{ij})$ are verified.

Thus, for each tuple (i, j, t) where a nonlinear term is defined, we select $Z(\gamma^{mt}_{ij})$ intersect points for the function to linearize. Then, by using the derivative of the objective function term $Z(x^t_{ij}) = \tau^t_{ij} x^t_{ij} = T_{ff}\left[1 + \alpha\left(\frac{x^t_{ij}}{q_{pc}}\right)^{\beta}\right] x^t_{ij}$ with respect to x^t_{ij}, we found the tangents to each of the selected points.

Proposition 3.1. *$\forall(i,j) \in \bar{A}, \forall m \in \{1,\dots,M\}$ the slope a_{ij}^{tm} and the intercept b_{ij}^{tm} of the tangents are identified by:*

$$a_{ij}^{tm} = T_{ff}\left[1+\alpha(\beta+1)\left(\frac{\gamma_{ij}^{tm}}{q_{pc}}\right)^{\beta}\right] \tag{9}$$

$$b_{ij}^{tm} = -\alpha T_{ff}\beta\gamma_{ij}^{tm}\left(\frac{\gamma_{ij}^{tm}}{q_{pc}}\right)^{\beta} \tag{10}$$

Proof. The tangent in a point γ_{ij}^{tm} is computed by the equation

$$\frac{y - Z(\gamma_{ij}^{tm})}{x_{ij}^{t} - \gamma_{ij}^{tm}} = \frac{\partial Z}{\partial x_{ij}^{t}}(\gamma_{ij}^{tm})$$

from which we obtain

$$a_{ij}^{tm} = \frac{\partial Z}{\partial x_{ij}^{t}}(\gamma_{ij}^{tm})$$

and

$$b_{ij}^{tm} = Z(\gamma_{ij}^{tm}) - \frac{\partial Z}{\partial x_{ij}^{t}}(\gamma_{ij}^{tm})\gamma_{ij}^{tm}$$

Considering that

$$Z(x_{ij}^{t}) = T_{ff}\gamma_{ij}^{tm}\left[1+\alpha\left(\frac{x_{ij}^{t}}{q_{pc}}\right)^{\beta}\right]$$

and that

$$\frac{\partial Z}{\partial x_{ij}^{t}}(\gamma_{ij}^{tm}) = T_{ff}\gamma_{ij}^{tm}\left[1+\alpha(\beta+1)\left(\frac{\gamma_{ij}^{tm}}{q_{pc}}\right)^{\beta}\right]$$

by simple algebraic steps we obtain the Eqs. (9) and (10) □

3.4. Upper approximation

Under the same conditions of 3.5 we can define a piecewise linear approximation where the terms γ_{ij}^{tm} of Definition 3.1 and the tuples $(a_{ij}^{mt}, b_{ij}^{mt})$ defining the lines in 3.2 are such that:

$$a_{ijt}^{m}\gamma_{ij}^{tm} + b_{ij}^{mt} = Z(\gamma_{ij}^{tm}) \tag{11}$$

$$a_{ijt}^{m}\gamma_{ij}^{tm+1} + b_{ij}^{mt} = Z(\gamma_{ij}^{tm+1}) \tag{12}$$

From the convexity of Z we can deduce this secant approximation being an upper approximation of the original objective function. One advantage given by the upper approximation is the functionalities offered by modern solvers allowing the easy implementation of piecewise linear approximation directly in the model.

Fig. 3 shows an example of tangent approximation. Dashed lines in the figure represent the set of tangents computed and used to approximate the objective function term. As depicted, the lines are very close at the beginning and at end of the curve. Using a proper number of tangents, and intersect points, we can easily limit the error and have a very tight approximation as demonstrated in the test case. This result in a very powerful mean to introduce nonlinearity as representation of congestion while controlling the complexity of the model and its usability as decision support tool.

Therefore, we can define a set of linear functions $a_{ij}^{tm}x_{ij}^{t} + b_{ij}^{tm}$ as defined in 3.2 and demonstrated in 3.1, computed with the assumption 3.5. After the linearization we remove the assumption 3.5, so by setting back the integer property of x_{ij}^{t} we introduce the MILP model P2 as follows. The same procedure can be followed to model the upper approximation simply computing the line terms satisfying the Eqs. (11) and (12)

Model **P2**

$$\min Z = \sum_{t\in T}\sum_{(i,j)\in\bar{A}}\tau_{ij}^{t}x_{ij}^{t} + \sum_{t\in T}\sum_{(i,j)\in\bar{A}}z_{ij}^{t} \tag{13}$$

s.t.

$$\sum_{i\in\delta^{-}(j):\bar{t}=(t-\tau_{ij}^{\bar{t}})\geq 0} x_{ij}^{\bar{t}} + y_{j}^{t-1} = y_{j}^{t} + \sum_{k\in\delta^{+}(j)} x_{jk}^{t} + d_{j}^{t} \quad j\in N, t\in T \tag{3}'''$$

$$0 \leq y_{j}^{t} \leq \mathrm{cap}_{i} \qquad j\in N, t\in T \tag{4}'''$$

$$0 \leq x_{ij}^{t} \leq \mathrm{capA}_{ij}^{t} \qquad (i,j)\in A, t\in T \tag{5}'''$$

$$z_{ij}^{t} \geq a_{ij}^{mt}x_{ij}^{t} + b_{ij}^{mt} \qquad (a_{ij}^{mt}, b_{ij}^{mt}) \in M_{ij}^{t},\ (i,j)\in\bar{A}, t\in T \tag{14}$$

$$z_{ij}^{t} \geq 0,\ y_{j}^{t}, x_{ij}^{t} \in \mathbb{Z}^{\geq 0} \qquad (i,j)\in A, t\in T \tag{15}$$

In the objective function (13) the first term sum all the contributions of the linear arcs which are $\bar{A} = A \setminus \bar{A}$, while the second term represent the contribution of the non linear arcs, measured by the z variables. The variables z_{ij}^{t} and constraints set (14) in model **P2** are used to define the linearization as tangent approximation as just explained. Given that the $\tau_{ij}^{t}x_{ij}^{t}$ function is non decreasing convex, they are sufficient to define the approximation. We use this model in the study of the application case defined in the following section.

4. The case study

In this section we describe how the application case is addressed and how the baseline instance has been built. The aim is twofold. The first objective is to build an instance as close as possible to the real scenario which is going to be investigated once the terminal is fully operational. The second objective is to let the instance be replicable and scalable in order to test the model on larger instances and to modify parameters once the terminal is in production and further data can be easily collected.

The application case considers the forwarding of containers from a terminal located in the port of Vado Ligure that is part of the Port Authority of the Western Ligurian Sea, which also includes the ports of Genoa, Savona and Pra (see http://www.apmterminals.com/ for more details). Fig. 4 shows the map of the area where the APM-VL terminal is located. The port of Vado Ligure is connected to the northernmost part of Italy via the highway network, consisting of the A6 Savona–Turin highway, the Brennero highway via the A33 Cuneo–Asti, and the A10 coastal highway. The new built terminal is designed to host mega-ships. The expected throughput of the terminal, expressed in terms of number of containers handled per year, is about 800,000 TEUs. Unloaded containers from each mega-ship must be forwarded to inland destinations in a short time. The demand and the locations are derived from estimations done in the previous works of Ambrosino et al. (2018), and Musso and Sciomachen (2020). The forwarding destinations are reached by using trans-shipment nodes (with or without buffer capacity) where are located dry ports or important shipment crossroads. The source points, buffers, and gate points of the container terminal enrich the selection of nodes. The gate points play an important role in the model because they are used to represent scenarios with flow dependent traveling times and congestion effects for the baseline instance. These data of the application case are reported in Table 1. The table reports, for each node of the network, the identification number, the name, the information if the node is a source, or a target (destination) node, the capacity, and the required demand. A negative value for the demand column denotes a source node. The total demand indicated in Table 1 is estimated to be of 2500 TEU per day, taking into account data from previous works, which estimate a total of 900,000 TEU over 360 days. These real case data are very important to validate the model as a decision support tool, and can be used to generate additional large scale instances if needed. For the planning of the containers' forwarding, we consider a time horizon $\mathcal{H}$ of 48 h horizon with a discretization

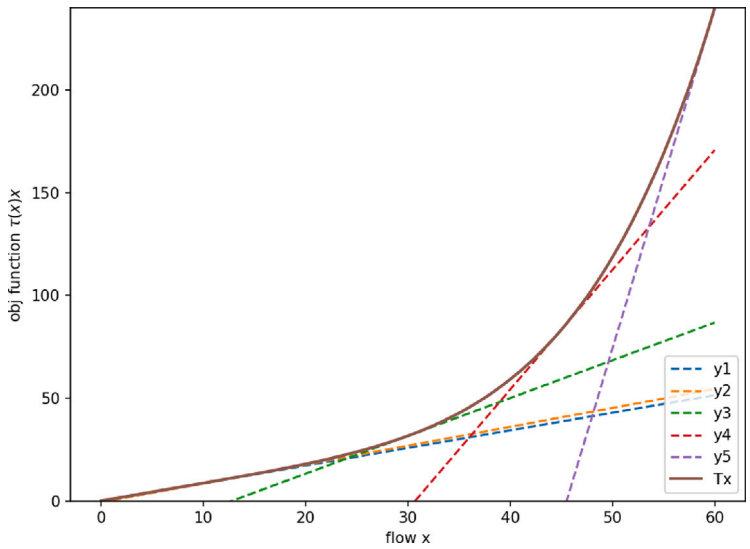

Fig. 3. Example of tangent approximation for convex polynomial term $\tau_{ij}^t x_{ij}^t$.

Fig. 4. Satellite view of Vado Ligure container terminal.

based on a time frame of 10 min ($TimeFrame$). The 10 min discretization guarantees the model to capture enough variations in traveling time registered by the traffic system. The traveling times have been computed by using the data of two different sources. The first one is the Open Source Routing Machine — OSRM (Luxen and Vetter, 2011), which has been used to compute the origin–destination distance matrix. The second one is Google Maps^{TM} used to compute information on max, min, and average traveling times extracted for each hour of the day of arcs. The arc capacity for the baseline instance has been set to $q_{pc} = TimeFrame * 60/10 = 60$ trucks every 10 min. In the baseline instance, the arc incident with the port gate is considered to follow the BPR function. As stated in definition 3.2, for that arc we have then linearization points such that $\gamma_{ij}^{t1} = 0$, and $\gamma_{ij}^{tM} = 60$. We set $M = 5$ (see Definition 3.1), considered the intersect points to be equidistant. In this case we have a linear function every $60/4 = 15$ units of flow. These settings resulted in a is a reasonable tradeoff between approximation and computational requirements.

4.1. Estimation of parameters

The estimation of the parameters has been made by considering several aspects of the case study related to the Vado Container terminal. Particular attention has been devoted to the estimation of the travel time τ_{ij}^t which, as already mentioned, can be assumed depending on day time, type of arc, and flow. We used Google Maps^{TM} web service to obtain the travel time for each hour of the day only for a selection of arcs because we wanted to extract a traveling time pattern which can be used to generate large instances without relying on the web service. Thus, we developed a procedure to extend to all other arcs the computation of traveling time, as explained in the following. The selected arcs are the ones incident with the terminal arc and others with different lengths, assuming that longer arcs have a higher average speed if compared to shorter ones. As can be noticed in the example of Fig. 5, the arcs connecting the terminal to Rivalta Scrivia and Genova (Genoa) are somehow shorter and have a higher fraction of their path on normal roads, leading to a lower speed, while arcs connecting it to farthest destinations, such as Ginevra (Geneva), and Ravenna, are characterized by a greater speed. After selecting arcs and divided them in these two groups, we queried the google web service in order to obtain the traveling time at each hour of the day. Then, we computed the relation time/distance for each hour of the day and type of arc in order to generate the travel time of the remaining arcs. For larger networks we can extract this information for a selection of arcs and apply it to other arcs, according to their classification, in order to estimate travel times.

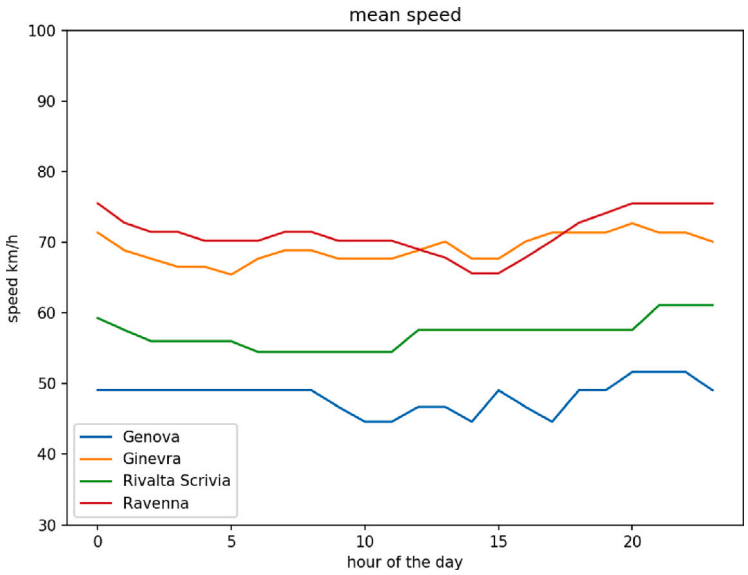

Fig. 5. Mean speed for a selection of arcs during the daytime.

Moreover, it is worth noting that, in respect of the travel times returned by the web services, a scale factor, $CarToTruck$ (CTT), is applied to consider the car to truck ratio, which is the reduction in speed of a truck if compared to the standard speed of a car. The estimation takes into account the maximum speed allowed, and our setting for the baseline instance is CTT = 0.8. Generally speaking, the value of CTT can be set considering the type of road and traveling rules applied to it. In particular, the maximum car speed in Italy along highway is 130 km/h, while for medium trucks (from 3.5 to 12 tons capacity) is 100 km/h and for heavy trucks (more than 12 tons capacity) is 80 km/h. Note that the trucks addressed in this study have a speed limit of 80 km/h, so the minimum value of CTT would be 0.6. This value is a lower bound and 0.8 would be a better estimation because not all the paths are on highway. Moreover, the average speed for cars are lower than 130 km/h while trucks tend to stay to their maximum allowed speed. The data obtained by the google map and OpenStreetMap web services allowed also to set the parameters for the BPR function (1). The parameters are T_{ff}, q_{pc}, α, and β. In order to compute these parameters, we need the estimation of the maximum and minimum speed s_{max}, s_{min} and the maximum traveling time T_{max} for a given arc in which we want to model the BPR function. The estimation of the traveling time for free flow and for T_{max} are, respectively, $T_{ff} = 60(dist/1000)/s_{max}$, and

$$T_{max} = T_{ff}(s_{max}/s_{min}) \tag{16}$$

The estimation of the parameters q_{pc}, α, and β has been done by looking to recent literature results such as those found by Lu et al. (2016) and by matching them with the available data for our case study. The maximum arc capacity q_{pc} has been set to 360 trucks per hour (6 trucks per minute); therefore the $TimeFrame$ is 60 trucks every 10 min.

The literature consider $\beta \approx 4$. For the purpose of our application we tested different values of α and we were able to put it in relation with T_{max} and T_{ff}, defining as the most appropriate value of α to be as in Eq. (17):

$$\alpha = \frac{T_{max}}{T_{ff}} - 1 \tag{17}$$

Eq. (17) in our setting is congruent with the estimations found by Lu et al. (2016). For the purpose of our model, in the case of $T_{max} = T_{ff}$, from Eq. (17) we obtain $\alpha = 0$, and then, from Eq. (1) $\tau = T_{ff}$, meaning that we have a linear model for traveling time. As opposite, if we suppose a maximum speed of 70 km/h and a minimum speed of 15 km/h (as we assumed for nonlinear terms, also thanks to the available data), considering Eqs. (16) and (17), we will get $\alpha = 70/15 - 1 = 3.67$. While these equations and these procedures to generate data are proved to be very useful and realistic, it is clear that future followups of this work will benefit of more proper data analytics based estimations with the VADO ligure system data available.

Table 1
Node list, buffer capacity, and demand of the baseline instance.

id	Name	Source	Target	Capacity	Demand
1	Vado Ligure	Y	N	0	−5000
2	Buffer Terminal 1	N	N	5000	0
3	gate enter	N	N	0	0
4	gate exit	N	N	0	0
5	Alessandria	N	N	1000	0
6	Novi Ligure	N	N	1000	0
7	Rivalta scrivia	N	N	2500	0
8	Piacenza	N	N	2500	0
9	Novara	N	N	2500	0
10	Parma	N	N	2500	0
11	Rubiera	N	N	2500	0
12	Bologna	N	N	2500	0
13	Torino	N	Y	2500	1285
14	Milano	N	Y	2500	760
15	Genova	N	Y	2500	465
16	Varese	N	Y	2500	455
17	Ravenna	N	Y	2500	310
18	Roma (Orte)	N	Y	2500	205
19	Cuneo	N	Y	2500	180
20	Ginevra	N	Y	2500	1340

5. Experimental results

Model P2 has been implemented in Gurobi™ 8.0, python interfaces 3.6.9 on Ubuntu 16.04 64 bit. The computing machine used in our computational experimentation is an Intel Core™ model i7-5600U CPU with 2.60 GHZ, RAM 8 GB. The maximum running time was set to 200 s. The baseline instance produced a MIP model of 7200 rows, 91 316 columns and 167 354 non-zeros elements which was solved in less than 10 s.

5.1. Validation of the model

The first analysis has been devoted to the linearization. After tuning, we used 5 linearization points for each nonlinear objective term; the

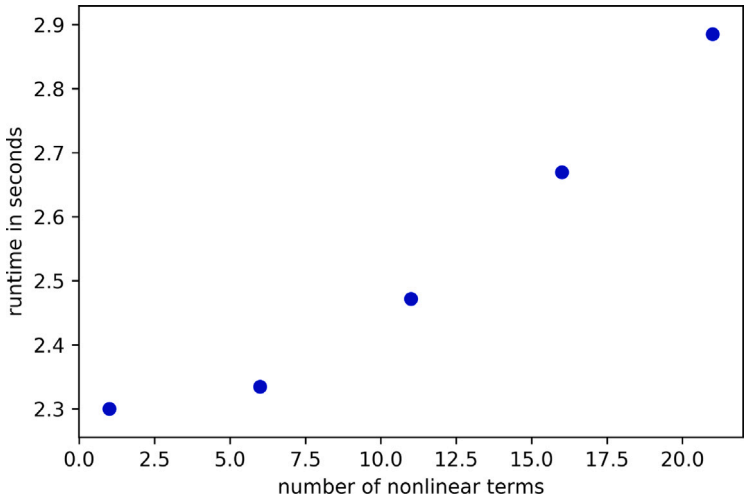

Fig. 6. Model runtime in the baseline instance when changing the number of nonlinear terms considered, and linearized with tangent approximation.

linearization always allowed obtaining a light model easily to solve with modern solvers and with a detailed approximation level. In order to check how the tangent approximation affected the solution, we compared it with the upper approximation described in Section 3.4, obtained with piece-wise linear functions intersecting the nonlinear terms at the same points where the lower approximation has been done with tangents. The gap between the aforementioned approximations is very tight, and less than 0.5% while considering from 1 to 22 nonlinear terms in the objective function. This means that we modeled progressively more arcs as nonlinear. We have to point out that considering more nonlinear terms in the studied instance is not useful as congestion is only well represented in the neighborhood of the terminal gate. With regard to computational time, we noticed a remarkable increase as depicted in the plot in Fig. 6; nevertheless, this increase is very far to make the computational time a concern.

In order to prove the validity of the model a further comparison has been made against a well consolidated modeling technique which considers explicitly time–space links. The model is derived by the one described in detail in Carey and Subrahmanian (2000). We report in the following the model named **P3**, with explicit consideration of the BPR function. This approach considers a wise selection of intersection points in order to have integer values for traveling time. In this case we have the variable $x_{ijt\tau}$ being the number of vehicles entering in arc (i,j) at time t, incurring in a travel time τ. The hypotesys is that the traveling time is a convex function of the flow and specifically is defined by the BPR Function. So we define a discrete traveling time $\tau \in \{t,\dots,T\} = \mathcal{T}$ from a set of points $\bar{x}_{ijt\tau}$ such that

$$\bar{x}_{ijt\tau} = \mathrm{BPR}^{-1}((i,j),t,\tau) = q_{pc}\sqrt[\beta]{\frac{1}{\alpha}\left[\frac{\tau}{T_{ff}}-1\right]} \tag{18}$$

The traveling time τ is different based on (i,j) and t, and this because T_{ff} and q_{pc} varies for each arc and for each timeperiod. While for arcs $(i,j) \in \tilde{A}$, where traveling time is modeled linearly, the notation τ_{ij}^t is left unchanged, for arcs $(i,j) \in \bar{A}$ we can explicit the relation between traveling time and flow. By Eq. (1) it is easy to derive extreme points for traveling time that are indeed $\tau_{min} = T_{ff}$ and $\tau_{max} = T_{ff}(1+\alpha)$, respectively. In order to linearize the convex function the variables $0 \le \lambda_{ijt\tau} \le 1, (i,j) \in \bar{A}, t \in \mathcal{T}$, $\tau \in \{\tau_{min},\dots,\tau_{max}\}$ are introduced, alongwith the following constraints

$$\sum_{\tau=\tau_{min}}^{\tau_{max}} \lambda_{ijt\tau} = 1 \qquad \forall ij \in \bar{A}, t \in \mathcal{T} \tag{19}$$

Being the BPR function convex, we do not need to write the Special Order Set constraints to model the piece-wise linear approximation (Bazaraa et al., 2013). Moreover Eq. (19) will be reduced to less or equal to 1 equation. Appliying the transormation to the traveling time, it can be written as

$$\mathrm{BPR}(x_{ijt\tau}) = \sum_{\tau=\tau_{min}}^{\tau_{max}} \lambda_{ijt\tau}\mathrm{BPR}(\bar{x}_{ijt\tau}) = \sum_{\tau=\tau_{min}}^{\tau_{max}} \tau\lambda_{ijt\tau} \tag{20}$$

and for each timeslot t we can obtain the quantitiy of flow traveling arc (i,j) by the following term:

$$\mathrm{flow}(i,j,t) = \mathrm{BPR}^{-1}(i,j,\tau) = \sum_{\tau=\tau_{min}}^{\tau_{max}} \bar{x}_{ijt\tau}\lambda_{ijt\tau} \tag{21}$$

The use of τ_{min} and τ_{max} implies a reduction of variables and constraints to be defined. Moreover the term (21) can be added in objective function multiplied by τ.

The model can be reformulated as follows: Model **P3**

$$\min\ Z = \sum_{(i,j)\in\tilde{A}}\sum_{t=1}^{T}\tau_{ij}^t x_{ij}^t + \sum_{(i,j)\in\bar{A}}\sum_{t=1}^{T}\sum_{\tau=\tau_{min}}^{\tau_{max}}\tau\bar{x}_{ijt\tau}\lambda_{ijt\tau} \tag{22}$$

$s.t.$

$$\sum_{(i,j)\in\bar{A}}\sum_{\tau=\tau_{min};t-\tau>0}^{\tau_{max}}\bar{x}_{ij(t-\tau)\tau}\lambda_{ij(t-\tau)\tau} + \sum_{(i,j)\in\tilde{A},\bar{t}=(t-\tau_{ij}^t),\bar{t}\ge 0} x_{ij}^{\bar{t}} + y_j^{t-1}$$
$$= y_j^t + \sum_{(j,k)\in\bar{A}}\sum_{\tau=\tau_{min};t+\tau\le T}^{\tau_{max}} x_{jkt\tau}\lambda_{jkt\tau} + \sum_{(j,k)\in\tilde{A}} x_{jk}^t + d_j^t \quad j\in N, t\in\mathcal{T} \tag{23}$$

$$0 \le y_j^t \le \mathrm{cap}_i \qquad j\in N, t\in\mathcal{T} \qquad (4)'''$$

$$0 \le x_{ij}^t \le \mathrm{capA}_{ij}^t \qquad (i,j)\in A, t\in\mathcal{T} \qquad (5)'''$$

$$\sum_{\tau=\tau_{min};t-\tau>0}^{\tau_{max}}\lambda_{ij(t-\tau)\tau} \le 1 \qquad (i,j)\in\bar{A}, t\in\mathcal{T} \tag{24}$$

$$\sum_{\tau=\tau_{min};\tau+t\le T}^{\tau_{max}}\lambda_{ijt\tau} \le 1 \qquad (i,j)\in\bar{A}, t\in T \tag{25}$$

$$y_j^t \in \mathbb{Z}^{\ge 0} \qquad (i,j)\in A, t\in\mathcal{T} \tag{26}$$

$$x_{ij}^t \in \mathbb{Z}^{\ge 0} \qquad (i,j)\in\tilde{A}, t\in\mathcal{T} \tag{27}$$

$$0 \le \lambda_{ijt\tau} \le 1 \qquad (i,j)\in\bar{A},\ t,\tau\in\mathcal{T} \tag{28}$$

The model can be used to validate the our proposed model in terms of computation time and objective function. We tested it in the same

Table 2
Performance comparison between **P2** model and **P3** model.

Model	Nodes	$\|A\|$	T	# nlarcs	objval	P3 vs. P2	Time	Gap
P2	10	46	6 h	2	1 054	3.01%	0.03	0.00%
P3	10	46	6 h	2	1 087		0.15	0.00%
P2	10	46	6 h	46	1 098	3.26%	0.05	0.00%
P3	10	46	6 h	46	1 135		20.00	0.00%
P2	20	276	48 h	2	51 520	2.22%	2.03	0.00%
P3	20	276	48 h	2	52 690		4.12	0.00%
P2	40	1336	48 h	26	87 753	2.96%	35.68	0.00%
P3	40	1336	48 h	26	90 428		1800.00	0.21%

conditions of our studied case. We refined the model implementation allowing a tunable number of breakpoints, in order to reduce the number of variables generated. In particular we tested with the same number of breakpoints used for the **P2** model. The results are depicted in Table 2. The table reports, for each row, the table name, the number of instance nodes, the number of arcs, the time horizon in hours, the number of non linear arcs considered, the objective value, the percentage of difference between the **P3** and the **P2** models, the computation time in seconds (with a maximum computational time set to 1800), and the gap. As expected, the **P3** model is an upper extimation of the **P2** model, but the gap between model is always limited to a maximum of 3.26% which is acceptable for planning purpose. Moreover, this type of gap is not growing with the growing of the instance. With respect to computational time model **P3** tends to take higher times to close for bigger instances. In this regard, results validate the choice to use the **P2** model over the **P3** model, in particular if we intend to use it inside frameworks where fast computational time can be important.

5.2. Analysis of buffer capacity

The second part of the test campaign has been devoted to validate the model as a decision support tool for the port authority. The model has been tested to analyze the effect of different parameters on congestion and overall model performance. By using the base settings as described in the previous section, also named the baseline instance, we firstly investigated the impact of the buffer capacity on both the congestion (i.e. the objective function) and the running time. To do so we changed the capacity of the buffers, which are listed in the fifth column of Table 1, generating different instances. The new buffer capacity is progressively set from 50% of the original capacity to 250% of the original capacity. To identify the instances, we introduce the parameter "cap factor" which is the ratio between the new buffer capacity and the original buffer capacity. The results demonstrate that, in the 48 h planning horizon, the capacity of the buffers in the baseline instance is enough to manage the congestion and only a reduction of 50% of the capacity affects the performance. The results are depicted in Fig. 7.

5.3. Considering shutdown hours

Another important issue to consider in our study and a critical decision for managers, is the potential shut-down of the gates during night shifts, when inland forwarding is planned. In the formulation this feature can be modeled by adding constraints of shutdown. This means that, given the set $\mathcal{T}^s$ of timeslot for which is forbidden to operate the terminal, and let $\mathcal{G}$ the set of arcs representing the gate of the terminal, then the following contraint is added to the formulation

$$x_{ijt} = 0 \quad \forall (i,j) \in \mathcal{G}, \forall t \in \mathcal{T}^s \tag{29}$$

For the purpose of the real case analysis, we considered three test scenario: no shut-down, 4 h shut-down, and 8 h shut-down. As expected, the congestion rise over in these three scenarios, as plotted in Fig. 8. The results when the hours of shut-down are changed can be also analyzed in detail and for each single arc. These results are described in Fig. 9 where the plots report the number of arcs in which the number of truck traveling that arcs are respectively less of 15, from 15 to 30, from 30 to 45, and from 45 to 60 (maximum capacity). The plottetd bars compare the levels for the three scenario of shutdown and show a notable difference between the "no shutdown" scenario with the respect the other shutdown scenarios. So it seems that, in these particular setting, the 23 pm to 4 am shutdown scenario seems the more effective one in terms of ratio congestion increase/availability.

5.4. Tests on arc capacity

Another analysis considers the variation of the arc capacity from its standard settings of 60 vehicles per 10 min considered in the baseline instance. In this test campaign, we progressively augmented the arc capacity from 20 to 120 vehicles per 10 min. The results are depicted in Fig. 10, which plots the optimal solution (measuring the congestion) when the arc capacity varies. As demonstrated by the results, a reduction of the standard capacity may highly affect the overall congestion while, as expected, no effects are reported if we augment too much the arc capacity. However, it is important to notice that in these experiments the nonlinearity is considered only at the arc representing the gate.

5.5. Results on country wide instance

In order to monitor the computational results with bigger instances an experiment on a 40 nodes instance, covering main logistics points on the nation of Italy has been developed. The instance is generated starting by the 20 nodes one. The increment of computational time is more then proportional to the increase of instance dimension and this behavior is emphasized by the non linear terms. The graph in Fig. 11 depicts this behavior where differences in computational time grow with the increase of non linear terms. The Figure compares execution time both of the upper approximation and the lower approximation. The results show a better time performance for the upper approximation. This is be justified by the more efficient implementation of the piecewise linear functions by the solver, and the fact that the intersect points are integer in the upper approximation while they are not in the lower approximation (in lower approximation case the tangent points are integer but not the intersect of the lines). We measured also the gap between the upper and lower approximation and it remains always below 0.4% for the instance of 40 nodes (decreasing in percentage if compared to the 0.5% of the 20 nodes instance). A further experiment has been conducted considering all the arcs as non linear. In this case, while the baseline instance is solved in 64.84 s, the country wide instance cannot be solved in the time limit and no feasible solution is found. However we must recall that we can realistically identify the impact of the non linear component of the traveling times due to the inland forwarding containers only in the surrounding of the port.

6. Conclusion

In this paper we discussed a mixed integer programming model for planning the inland forwarding of containers unloaded by mega-ships. The aim is to give a support to the planners in order to minimize congestion effects caused by mega-ship trend and the need to dislocate containers in short time. The inland forwarding with congestion can be classified as a "first mile" logistics problem and may cause errors in planning if not accounted correctly; the modeling of travel time is critical in order to represent and control congestion effects. Congestion can be considered only if nonlinear terms are represented in the model. Nonlinear terms may cause complexities in the model which can be managed by using linearization and mixed integer programming. Our proposed tangent approximation allowed to maintain the model easy to be solved with a very tight gap if compared with upper bounds. As a result, our approach allowed to produce a light model which

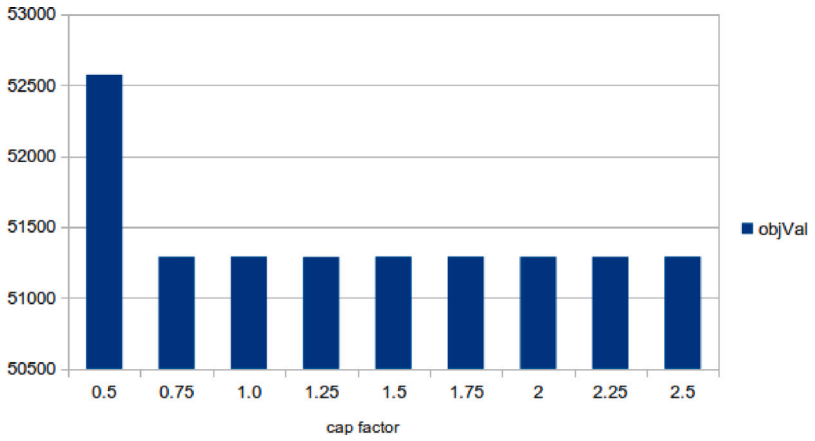

Fig. 7. Object value for the optimal solution of P2 model when capacity of buffers changes. In abscissa "cap factor" is the ratio between the capacity of the buffers of the considered instance and the capacity of the buffers in the baseline instance. "cap factor" equal to 1 stands for the baseline instance.

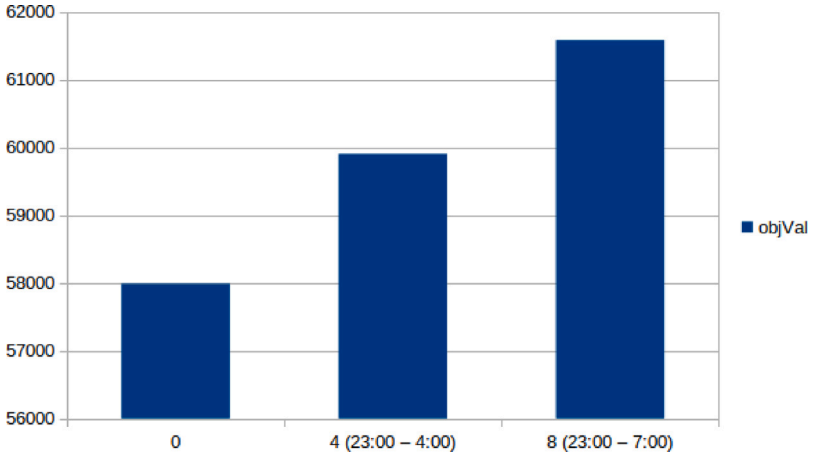

Fig. 8. Congestion with different gate shut-down scenarios.

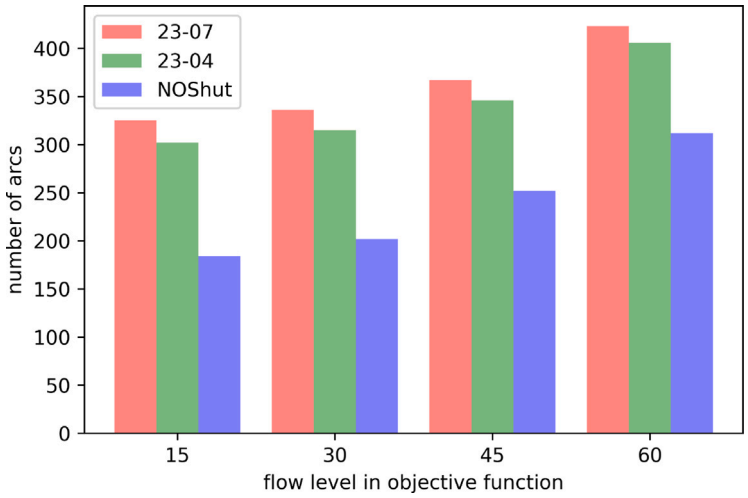

Fig. 9. Impact of shutdown hours on objective: number of arcs having flow level from 15 to 60 for each shutdown scenario.

can be effectively used for macro planning of forwarding operations. The model is proved to be computationally faster of classical literature approaches in real case instaces. The application case is the Container Terminal of VADO Ligure, which is going to be the main Italian hub for mega-ships. We used different studies and data sources in order to design the baseline instance of a 48 h planning problem. The parameters of the model have been systematically defined by integrating studies on containers to be handled in the VADO Ligure container terminal,

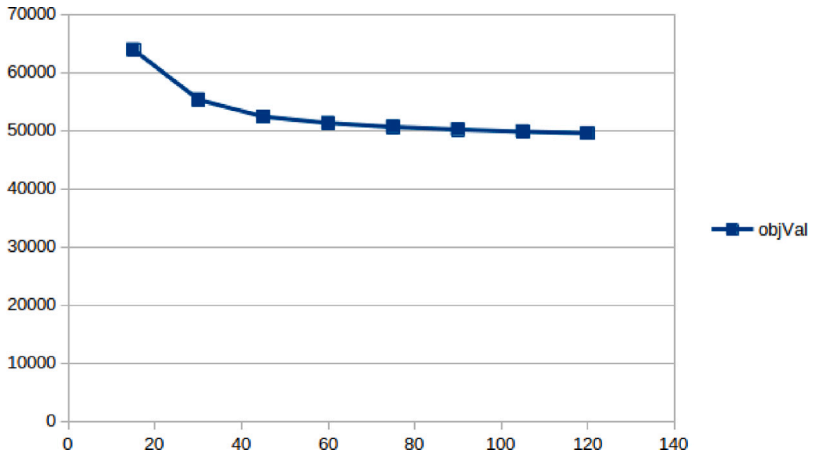

Fig. 10. Congestion related to arc capacity in vehicles per 10 min.

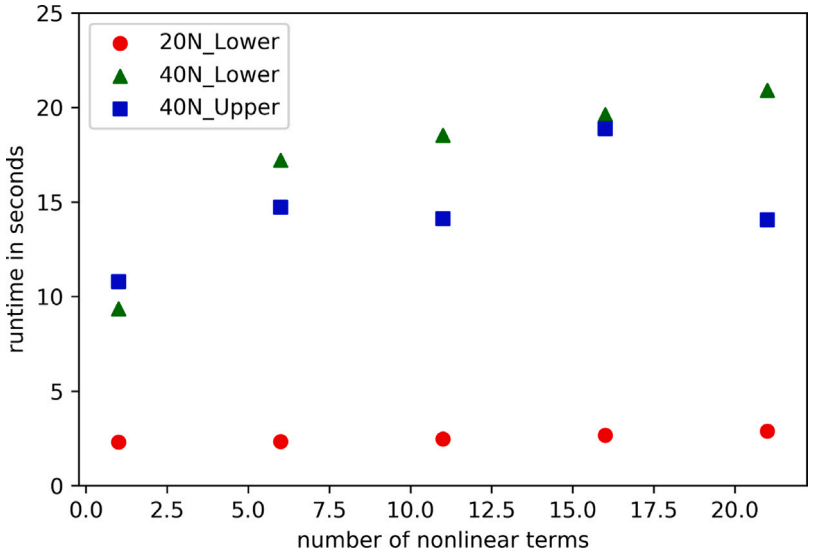

Fig. 11. Model runtime in the 40 nodes instance (40 N) compared with the 20 nodes instance (20 N) when changing the number of nonlinear terms considered, and linearized with tangent approximation.

by studying the literature on congestion functions, and by studying the map and the data available on well known map services (such as Google Maps™ and OpenStreetMap). We were able to find relations on the parameters which allow to generalize their estimations thus facing the traveling time function in a simpler way than in other previous methods proposed in the recent literature. Starting from the implemented instance we tested the behavior of the model under different scenarios. In particular, we found the importance of controlling shutdown hours in order to lower congestion. Other test results confirmed congestion peaks that can be caused by reductions in buffer and arc capacities. As a followup of this work we are going into three main directions. First, we think it is important to integrate the consideration of environmental impact. Further, from this general model a more detailed multicommodity one can be derived when detailed data will be available, and in this case fleet service allocation models considering congestion can be formulated. Finally, a simulation–optimization approach, not yet presented in the literature in this field, is in progress to better synchronize the arrivals of the containers at the terminal with their inland forwarding.

CRediT authorship contribution statement

Anna Sciomachen: Conceptualization, Methodology, Data curation, Writing and editing, Mathematical model, Validation. **Giuseppe Stecca:** Conceptualization, Methodology, Writing and editing, Mathematical model, Software, Validation.

Declaration of competing interest

The authors declare that they have no known competing financial interests or personal relationships that could have appeared to influence the work reported in this paper.

Data availability

Data will be made available on request.

Acknowledgments

This work has been partially supported by NextGeneration EU/ Italian Ministry of University and Research MUR Missione 4 Componente 2, Investimento 1.4 — D.D. 1033 17/06/2022 grant id

CN00000023, PNRR Sustainable Mobility Center (Centro Nazionale per la Mobilità Sostenibile — CN MOST), CUP number B43C22000440001. This manuscript reflects only the authors' views and opinions, neither the European Union nor the European Commission can be considered responsible for them. The work has also been partially supported by RAISE — Robotics and AI for Socio-economic Empowerment Ecosistema dell'Innovazione della Liguria, PNRR — M4C2 — I1.5 — ECS00000035 Spoke 4 "Smart and sustainable ports".

References

Alizadeh, M., Wai, H.-T., Scaglione, A., Goldsmith, A., Fan, Y.Y., Javidi, T., 2014. Optimized path planning for electric vehicle routing and charging. In: 2014 52nd Annual Allerton Conference on Communication, Control, and Computing (Allerton). IEEE, pp. 25–32.

Ambrosino, D., Ferrari, C., Sciomachen, A., Tei, A., 2018. Ports, external costs, and Northern Italian transport network design: effects for the planned transformation. Marit. Policy Manag. 45 (6), 803–818.

Ambrosino, D., Sciomachen, A., Surace, C., 2019. Evaluation of flow dependent external costs in freight logistics networks. Networks 74 (2), 111–123.

Bazaraa, M.S., Sherali, H.D., Shetty, C.M., 2013. Nonlinear Programming: Theory and Algorithms. John Wiley & Sons.

Birge, J.R., Ho, J.K., 1993. Optimal flows in stochastic dynamic networks with congestion. Oper. Res. 41 (1), 203–216.

Brandenburg, M., Govindan, K., Sarkis, J., Seuring, S., 2014. Quantitative models for sustainable supply chain management: Developments and directions. European J. Oper. Res. 233 (2), 299–312.

Carey, M., 1992. Nonconvexity of the dynamic traffic assignment problem. Transp. Res. B 26 (2), 127–133.

Carey, M., Subrahmanian, E., 2000. An approach to modelling time-varying flows on congested networks. Transp. Res. B 34 (3), 157–183.

De Langen, P.W., Chouly, A., 2004. Hinterland access regimes in seaports. Eur. J. Transp. Infrastruct. Res. 4 (4), 361–380.

Di Francesco, M., Gentile, C., Schirra, S., Stecca, G., Zuddas, P., 2019. An integral LP relaxation for a drayage problem. Discrete Optim. 31, 93–102.

Essel, D., Jin, Z., Zang, L., Agyabeng-Mensah, Y., Afum, E., Baah, C., 2022. Assessing the impact of the Boankra inland container terminal on the operational performance of the seaports of Ghana. Res. Transp. Bus. Manag. 44, 100832.

Feng, X., Song, R., Yin, W., Yin, X., Zhang, R., 2023. Multimodal transportation network with cargo containerization technology: Advantages and challenges. Transp. Policy 132, 128–143.

Funke, J., Kopfer, H., 2016. A model for a multi-size inland container transportation problem. Transp. Res. E 89, 70–85.

Gelareh, S., Nickel, S., Pisinger, D., 2010. Liner shipping hub network design in a competitive environment. Transp. Res. E 46 (6), 991–1004.

Haralambides, H.E., 2019. Gigantism in container shipping, ports and global logistics: a timelapse into the future. Marit. Econ. Logist. 21 (1), 1–60.

Ishfaq, R., Sox, C.R., 2012. Design of intermodal logistics networks with hub delays. European J. Oper. Res. 220 (3), 629–641.

Jia, S., Cui, H., Chen, R., Meng, Q., 2022. Dynamic container drayage with uncertain request arrival times and service time windows. Transp. Res. B 166, 237–258.

Jia, S., Li, C.-L., Xu, Z., 2020. A simulation optimization method for deep-sea vessel berth planning and feeder arrival scheduling at a container port. Transp. Res. B 142, 174–196.

Karimi-Mamaghan, M., Mohammadi, M., Pirayesh, A., Karimi-Mamaghan, A.M., Irani, H., 2020. Hub-and-spoke network design under congestion: A learning based metaheuristic. Transp. Res. E 142, 102069.

Korzhenevych, A., Dehnen, N., Bröcker, J., Holtkamp, M., Meier, H., Gibson, G., Varma, A., Cox, V., 2014. Update of the Handbook on External Costs of Transport: Final Report for the European Commission. DG-MOVE.

Kramberger, T., Monios, J., 2018. Using dry ports for port co-opetition: the case of Adriatic ports. Int. J. Shipp. Transp. Logist. 10 (1), 18–44.

Kurt, I., Aymelek, M., Boulougouris, E., Turan, O., 2021. Operational cost analysis for a container shipping network integrated with offshore container port system: A case study on the West Coast of North America. Mar. Policy 126, 104–400.

Kurtuluş, E., 2022. Optimizing inland container logistics and dry port location-allocation from an environmental perspective. Res. Transp. Bus. Manag. 100839.

Li, X., Xie, C., Bao, Z., 2022. A multimodal multicommodity network equilibrium model with service capacity and bottleneck congestion for China-Europe containerized freight flows. Transp. Res. E 164, 102786.

Lu, Z., Meng, Q., Gomes, G., 2016. Estimating link travel time functions for heterogeneous traffic flows on freeways. J. Adv. Transp. 50 (8), 1683–1698.

Luxen, D., Vetter, C., 2011. Real-time routing with OpenStreetMap data. In: Proceedings of the 19th ACM SIGSPATIAL International Conference on Advances in Geographic Information Systems. GIS '11, ACM, New York, NY, USA, pp. 513–516. http://dx.doi.org/10.1145/2093973.2094062, URL: http://doi.acm.org/10.1145/2093973.2094062.

Maerivoet, S., De Moor, B., 2005. Transportation planning and traffic flow models. arXiv preprint physics/0507127.

Manual, T.A., 1964. Urban Planning Division. US Department of Commerce, Washington DC.

Medina, J., Kim, J.-H., Lee, E.S., 2021. Did the Panama Canal expansion benefit small US ports? Marit. Transp. Res. 2, 100013.

Merchant, D.K., Nemhauser, G.L., 1978. A model and an algorithm for the dynamic traffic assignment problems. Transp. Sci. 12 (3), 183–199.

Mostert, M., Caris, A., Limbourg, A., 2017. Road and intermodal transport performance: the impact of operational costs and air pollution external costs. Res. Transp. Bus. Manag. 23, 57–85.

Musso, E., Sciomachen, A., 2020. Impact of megaships on the performance of port container terminals. Marit. Econ. Logist. 22 (3), 432–445.

Notteboom, T., Rodrigue, J., 2008. Containerization, box logistics and global supply chains: the integration of ports and liner shipping networks. Marit. Econ. Logist. 10 (1), 152–174.

Papageorgiou, M., 1990. Dynamic modeling, assignment, and route guidance in traffic networks. Transp. Res. B 24 (6), 471–495. http://dx.doi.org/10.1016/0191-2615(90)90041-V.

Peeta, S., Ziliaskopoulos, A.K., 2001. Foundations of dynamic traffic assignment: The past, the present and the future. Netw. Spat. Econ. 1 (3), 233–265. http://dx.doi.org/10.1023/A:1012827724856.

Petro, F., Konečnỳ, V., 2017. Calculation of emissions from transport services and their use for the internalisation of external costs in road transport. Procedia Eng. 192, 677–682.

Roso, V., Lumsden, K., 2010. A review of dry ports. Marit. Econ. Logist. 12, 196–213.

dos Santos, M.C., Pereira, F.H., 2021. Development and application of a dynamic model for road port access and its impacts on port-city relationship indicators. J. Transp. Geogr. 96, 103–189.

Sterzik, S., Kopfer, H., 2013. A tabu search heuristic for the inland container transportation problem. Comput. Oper. Res. 40 (4), 953–962.

Tawfik, C., Limbourg, S., 2019. Scenario-based analysis for intermodal transport in the context of service network design models. Transp. Res. Interdiscip. Perspect. 2, 100036. http://dx.doi.org/10.1016/j.trip.2019.100036.

Wang, T., Tian, X., Wang, Y., 2020. Container slot allocation and dynamic pricing of time-sensitive cargoes considering port congestion and uncertain demand. Transp. Res. E 144, 102149.

Yu, M., Fransoo, J.C., Lee, C.-Y., 2018. Detention decisions for empty containers in the hinterland transportation system. Transp. Res. B 110, 188–208.